Europe PMC Funders Group
Author Manuscript
Clin Cancer Res. Author manuscript; available in PMC 2012 May 15.

Published in final edited form as:
Clin Cancer Res. 2011 November 15; 17(22): 7003–7014. doi:10.1158/1078-0432.CCR-11-1870.

Novel Chromosomal Rearrangements and breakpoints at the t(6;9) in Salivary Adenoid Cystic Carcinoma: association with *MYB-NFIB* chimeric fusion, *MYB* expression, and clinical outcome

Yoshitsugu Mitani[1], **Pulivarthi H. Rao**[2], **P. Andrew Futreal**[3], **Dianna B. Roberts**[4], **Philip J. Stephens**[3], **Yi-Jue Zhao**[2], **Li Zhang**[5], **Mutsumi Mitani**[1], **Randal S. Weber**[4], **Scott M. Lippman**[6], **Carlos Caulin**[4], and **Adel K. El-Naggar**[1,4]

[1]Department of Pathology, The University of Texas MD Anderson Cancer Center, Houston, Texas

[2]Department of Pediatrics, Baylor College of Medicine, Houston, Texas

[3]Cancer Genome Project, The Wellcome Trust Sanger Institute, Hinxton, Cambridge, United Kingdom

[4]Department of Head and Neck Surgery, The University of Texas MD Anderson Cancer Center, Houston, Texas

[5]Department of Bioinformatics and Computational Biology, The University of Texas MD Anderson Cancer Center, Houston, Texas

[6]Department of Thoracic/Head and Neck Medical Oncology, The University of Texas MD Anderson Cancer Center, Houston, Texas

Abstract

Objective—To investigate the molecular-genetic heterogeneity associated with the t(6:9) in adenoid cystic carcinoma (ACC) and correlate the findings with patient clinical outcome.

Experimental Design—Multi-molecular and genetic techniques complemented with massive pair-ended sequencing and SNP array analyses were used on tumor specimens from 30 new and 52 previously RT-PCR analyzed fusion transcript negative ACCs. *MYB* mRNA expression level was determined by quantitative RT-PCR. The results of 102 tumors (30 new and 72 previously reported cases) were correlated with the clinicopathologic factors and patients' survival.

Results—The FISH analysis showed 34/82 (41.5%) fusion positive tumors and molecular techniques identified fusion transcripts in 21 of the 82 (25.6%) tumors. Detailed FISH analysis of 11 out the 15 tumors with gene fusion without transcript formation showed translocation of *NFIB* sequences to proximal or distal sites of the *MYB* gene. Massive pair-end sequencing of a subset of tumors confirmed the proximal translocation to an *NFIB* sequence and led to the identification of a new fusion gene (*NFIB*-AIG1) in one of the tumors. Overall, *MYB-NFIB* gene fusion rate by FISH was in 52.9% while fusion transcript forming incidence was 38.2%. Significant statistical association between the 5′ *MYB* transcript expression and patient survival was found.

Corresponding Author: Adel K El-Naggar, MD, PhD, Department of Pathology, Unit 85, The University of Texas M. D. Anderson Cancer Center, 1515 Holcombe Blvd., Houston, TX, 77030-4009, USA. Phone number: 713-792-3109, Fax number: 713-792-5532 anaggar@mdanderson.org.

Europe PMC Funders Author Manuscripts
Europe PMC Funders Author Manuscripts

Conclusions—We conclude that: 1) t(6;9) results in a complex genetic and molecular alterations in ACC, 2) *MYB-NFIB* gene fusion may not always be associated with chimeric transcript formation, 3) non-canonical *MYB, NFIB* gene fusions occur in a subset of tumors, 4) high *MYB* expression correlates with worse patient survival.

Keywords

Gene fusion; Gene fusion; chromosomal translocations; salivary gland carcinomas; molecular alterations

INTRODUCTION

Salivary adenoid cystic carcinoma, a relatively uncommon malignancy, is known for its progressive and heterogeneous clinical behavior (1-3). The primary treatment for patients with ACC is surgical resection with and without post-operative radiotherapy dependent upon the presence or the lack of adverse pathologic findings (4). More than 60% of these patients succumb to recurrent and/or metastatic disease with limited therapeutic options (4-6). Several recent genomic studies have attempted to unravel the events associated with ACC development and to identify molecular and biological markers for better management of patients with advanced disease (9, 12). Although no definitive marker(s) has been identified, recurrent loss of the terminal region of the long arm of chromosome 6 and translocation involving chromosomes 6q and 9p regions on different partners were the most consistently reported findings (7-13).

Recently, a fusion between the *MYB* and *NFIB* genes resulting from t(6;9)(q22-23;p24) regions have been identified in all 11 ACCs and were found to be associated with high 5′-*MYB* gene expression (14). Our group subsequently reported a lower incidence of *MYB-NFIB* fusion transcript, numerous fusion variants (15) and high level of the 5′-segment of the *MYB* transcript in the majority of fusion positive tumors. We also noted that a subset of fusion negative tumors express *MYB* level similar to those of fusion positive tumors. These observations, together with the complex fusion variants and the high incidence of *MYB-NFIB* gene fusion by in-situ hybridization (22), support the involvement of different molecular events associated with the t(6;9) in the *MYB* gene regulation (16-23) and other yet to be identified aberrations. We contend that accounting for these alterations is critical to understanding the role of the *MYB-NFIB* gene fusion in ACC development and progression.

To thoroughly account for the molecular genetic alterations associated with the t(6;9) in ACC and to understand their biological implications, we performed detailed cytogenetic and molecular analyses on 30 new ACCs and the 52 previously screened *MYB-NFIB* fusion transcript negative tumors and correlated the findings with the clinicopathologic parameters and the patient outcome.

MATERALS and METHODS

Tissue specimens and cohort analysis

We used fresh frozen tissue specimens from eighty-two primary ACCs accessioned at the head and neck section from 1989 to 2010 which comprised of 30 previously unanalyzed specimens and the 52 fusion transcript negative tumors from our earlier report (15). Tumors were classified into tubular and cribriform if they lacked any solid component and manifested at 75% of either form. (6) Tumors were categorized as solid if this feature is identified in any area. For clinical correlation of fusion positive and negative tumors, we also included all fusion positive tumors previously reported (15) for a combined total of 102 patients.

Europe PMC Funders Author Manuscripts
Europe PMC Funders Author Manuscripts

Europe PMC Funders Author Manuscripts

Europe PMC Funders Author Manuscripts

RNA extraction and fusion transcript sequencing

Total RNA was extracted with the TRIzol reagent (Invitrogen) and treated with recombinant DNase I, RNase-free (Roche) prior to RT-PCR and converted subsequently to cDNA using the SuperScript™ III First-Strand Synthesis System for RT-PCR (Invitrogen) with oligo(dt) primers according to the manufacturer's instructions. The amplification of the *MYB-NFIB* fusion transcripts and the primers used were described previously (Supplementary Table 1) (15). The *MYB-NFIB* fusion transcripts were detected by PCR analysis with Platinum Taq DNA polymerase (Invitrogen). We designed a new set of primers (Supplementary Table 1) in addition to the previously published primer sets (Supplementary Table 1). *ACTB* primer (Supplementary Table 1) was used as internal control. RT-PCR products were purified and sequenced directly or cloned into the pCR2.1 vector (Invitrogen). The PCR fragments were sequenced with an ABI PRISM 3130 Genetic Analyzer (Applied Biosystems) at the DNA sequencing core facility. The *MYB-NFIB* variants, the nucleotide sequences and genomic organization of *MYB* (accession number NM_001130173) and *NFIB* (ENSG00000147862) were determined using the NCBI (http://www.ncbi.nlm.nih.gov) and Ensemble (http://ensembl.org), respectively.

Quantitative RT-PCR

Quantitative RT-PCR was performed using the Applied Biosystems 7900HT Real-time PCR systems (Applied Biosystems) with Power SYBR® Green PCR Master Mix (Applied Biosystems). The primer sequences are shown in Supplementary Table 1. The *ACTB* gene was used as internal control. Duplicate samples for each tumor or tissue were analyzed. The expression of *MYB* transcripts were determined by the ΔCT method (Average CT-*MYB*-Average CT-*ACTB*), and relative *MYB* expression in each tumor was determined based on *MYB* expression in a pooled normal salivary gland standard (Clontech Laboratories). The average of each individual tumor and this value was used to determine the average for fusion positive and negative tumor groups. In this study, we considered the upper quartile of *MYB* values to represent the high expression.

Fluorescent *in situ* hybridization (FISH)

FISH was performed on touch preparations of ACCs to identify *MYB*/*NFIB* rearrangements. We initially used BAC clones containing *MYB* gene (RP11-104D9) and *NFIB* gene (RP11-54D21 and RP11-79B9) for screening of the gene fusion (Figure. 1A). The probes were labeled with Spectrum Green and Spectrum Red, respectively (Abbott Laboratories, Abbott Park, IL). Hybridization and detection were performed according to the manufacturer's protocols. 200 individual nuclei were analyzed for each case and the interphase nuclei was captured and processed using the Quantitative Image Processing System (Applied Imaging, Santa Clara, CA). In nuclei containing the *MYB-NFIB* fusion, green and red signals from the *MYB* and *NFIB* genes overlap in a red/green (yellow) signal.

To localize the alternate breakpoints in fusion positive transcript negative tumors, we selected two BAC clones; one at 5′ of *MYB* (RP11-378M4) and the other at 3′ of *MYB* gene (RP11-55H4). Both of these clones overlap with the *MYB* clone used in the first FISH (RP11-104D9) screening probe (Figure 3A).

3′ Rapid Amplification of cDNA Ends (3′RACE)

To determine the 3′ end of *MYB* transcript sequence or detect the unknown gene fusion of *MYB*, first-strand cDNA was synthesized 2μg of total RNA by M-MLV reverse transcriptase (Ambion) using 3′RACE adapter primer (AP; Invitrogen, Supplementary Table 1). 3′RACE nested PCR was done using 2 sets of *MYB* gene specific primers (Supplementary Table 1) and 3′RACE universal primer (AUAP; Invitrogen, Supplementary

Europe PMC Funders Author Manuscripts

Europe PMC Funders Author Manuscripts

Table 1) to generate a specific amplification product. PCR products were purified and sequenced directly or cloned into the pCR2.1 vector (Invitrogen), and then were sequenced.

DNA copy number analysis

Genomic DNA was extracted with Gentra Puregene Tissue Kit (QIAGEN) according to the manufacturer's instructions. DNA copy number (CN) from nineteen tumors and corresponding normal specimens was analyzed by affymetrix GeneChip Human Mapping 250k NSP array. The mapping information of the SNP sites was provided by the Human genome sequence version NCB136/hg18. Array data analyses were performed using Partek software and R packages.

Massive parallel sequencing

The procedures for genome wide paralleled paired-end sequencing to identify somatic genomic alterations and rearrangements in tumor specimens were performed as previously described (24, 25). Briefly, 5ug of genomic DNA from tumor and normal specimens were sheared to 400-500 bp fragments. Sequencing of 37 bp from either end was performed on the Illumina Genome Analyzer II platform. Reads were aligned to reference human genome (NCB1 build 36) using MAQ (26), with a coverage up to 1-2X sequence (50-60 million reads, 37 bp paired and N400 6p inserts), giving a physical coverage of 6-8X (25). Putative genomic rearrangements were screened by PCR across the breakpoint in tumor DNA samples and germline DNA (27).

Statistical analysis

Descriptive statistics for scaled values and frequencies of study patients within the categories for each of the parameters of interest were enumerated with the assistance of commercial statistical software. Correlations between categorical parameters and endpoints were assessed by Pearson's Chi-squared or, where there are fewer than ten subjects in any cell of a 2 × 2 grid, by the two-tailed Fisher exact test. Since the values for expression of *MYB* at exons 2-3 and at exons 15-16 did not meet tests for normality, possible differences between groups were assessed by the non-parametric Mann-Whitney U test. Curves describing overall survival were generated by the Kaplan-Meier product limit method. The statistical significance of differences between the actuarial curves was tested by the log rank test. Follow-up time was the time from first appointment at the University of Texas M. D. Anderson Cancer Center for the primary tumor of concern until the date of last contact or death. Proportional hazard ratios and multivariate models were assessed by Cox regression analysis. These statistical tests were performed with the assistance of the *Statistical* (StatSoft, Inc., Tulsa, OK) and SPSS (IBM SPSS, IBM Corporation, Somers, NY) statistical software applications.

RESULTS

In the initial phase of the study, we analyzed 30 new ACCs representing equal number of patients by multiple complementary techniques to account for heterogeneity of the molecular genetic alterations associated with the t(6;9). The patients comprised of 17 males and 13 females who ranged in age from 39 to 94 with a mean of 62 years. The tumor size ranged from 0.2 – 12.0 cm, with mean of 3.1 cm and twenty tumors (66.7%) had perineural invasion. All patients underwent surgical resection with curative intent and post-operative radiotherapy. Table 1 presents the genetic and molecular findings of 30 new ACCs by different techniques.

Europe PMC Funders Author Manuscripts

Europe PMC Funders Author Manuscripts

MYB-NFIB genomic translocation and fusion transcript of the 30 new ACCs

To screen for the *MYB-NFIB* gene fusion and the transcript formation, we performed FISH using BAC clones for the *MYB* gene (green, RP-11-104D9, Figure 1A) and the *NFIB* gene (red, RP11-54D21 and RP11-79B9, Figure 1A) and RT-PCR using the original set of and newly designed primers on all 30 tumors (Figure 1B) and all fusion PCR products were sequenced. None of the FISH negative tumors had fusion transcripts formation by RT-PCR. FISH analysis showed 17 (56.7%) tumors to be positive for the *MYB* and *NFIB* genes translocation (Table 1). Nine (52.9%) of the FISH positive samples had detectable fusion transcript and eight (26.7%) lacked transcript product (Figure 1C and Table 1); these data suggest that additional rearrangements or breakpoints other than *MYB-NFIB* fusions are present. Considering the complex and evolving information on the structural formation of the *MYB* gene, (27) we observed that exon 10 of the gene is lost in all sequenced *MYB-NFIB* chimeric transcript and the intact form of *MYB* transcript in ACC. This exon is also known as exon 9B, using NCBI accession #HSU22376.

To assess alteration at the 3′end of the *MYB* transcript, 3′RACE amplification was performed and led to the identification of three fusion transcripts; these were not detected by RT-PCR analysis (Table 1). Interestingly, two FISH positive tumors (#290F8 and 394D7, Figure 1D) had fusion transcripts comprised of *MYB* exon 15 and the 3′UTR of the *NFIB* gene and manifested the expected high level of *MYB* truncated transcript (Figure 1E and Supplementary Figure 1); one tumor (# 288F7) had fusion between *MYB* exon 13 and intron 22 of the *EFR3A* gene on chromosome 8q24 (Table 1 and Supplementary Figure 2); in addition to a stop codon at intron 13 and *MYB* truncated transcript.

MYB transcript expression

We previously reported loss or marked reduction of the full-length *MYB* (exon 15-16) transcript expression in all *MYB-NFIB* fusion positive tumors. To confirm this finding, we analyzed the expression levels of *MYB* transcripts in 30 salivary tumors by quantitative RT-PCR using primers for *MYB* exons 2-3 and the last *MYB* exon. Overall, the expression of *MYB* exon 2-3 in fusion transcript positive tumors (average 361) was more than two-fold higher than the majority of their fusion transcript negative ACCs (average 172) (Table 1). The analysis also shows that the expression levels of *MYB* exon 2-3 and the last exon were comparable in the majority of tumors with genomic *MYB-NFIB* fusion without transcript formation. In one tumor (#288F7, Table 1) with *MYB* and *EFR3A* gene fusion, the expression of the last *MYB* exon was markedly reduced while the 5′-segment was moderately elevated. We also observed that the three tumors with the highest 5′-segment *MYB* transcript (cases # 404D3, 369B5, and 133C4) had fusion between *MYB* exon 8b and exon 12 of *NFIB* gene (Figure 1F and Table 1).

Analysis of 52 fusion transcript negative of 72 ACCs previously studied

Based on these findings, we extended our analysis to include the 52 *MYB-NFIB* fusion transcript negative ACCs from our previous study (15). The analysis showed that seventeen (32.7%) of the 52 tumors to be positive for gene fusion by FISH, and only eight of these (6 by PCR and 2 by the 3′RACE) were *MYB/NFIB* transcript forming tumors (Table 1). Two of these tumors (542A1 and 318H3) had fusion between *MYB* exon 14 (Supplementary Figure 3) and intron 11 (Supplementary Figure 4) and the *NFIB* 3′UTR, respectively. In addition, we identified a novel t(6;9) rearrangement involving *MYB* exon15 and an inverted sequence of the *PDCD1LG2* intron 3 (Table 1 and Supplementary Figure 5) in another tumor (# 405B2). Another tumor (485F7) showed *MYB/NFIB* gene fusion by FISH but no transcript formation or *MYB* alterations was found (Figure 2A).

Europe PMC Funders Author Manuscripts

Europe PMC Funders Author Manuscripts

Detailed FISH analysis

To account for the translocation sites in gene fusion positive but transcript negative ACCs, we selected additional BAC clones at the 3′ and 5′ of the *MYB* gene that overlaps with the original *MYB* probe (Figure 3A). The results revealed, 5′ fusion signal proximal to the *MYB* gene in one tumor (Supplementary Table 2), a positive 3′ probe signals in eight, and fusion signals were found for both the 3′ and the 5′ flanking probes of the *MYB* in two tumors. Surprisingly, the two cases (288F7 and 405B2) where *MYB* fused with *EFR3A* or *PDCD1LG2* showed as a positive by 3′ probe signal suggesting that each allele fused different genes. These findings localize the breakpoints distal to the 3′ end of the *MYB* gene in 8 tumors and to the proximal 5′ end of the gene in one tumor. In the two tumors positive for both probes, either reciprocal translocation and/or translocation in one allele and insertion involving the other allele may have occurred. Detailed molecular analyses of these two tumors are underway.

Massively pair-ended sequencing analysis

To survey the genomic findings in tumors representing the *MYB-NFIB* gene fusion status, four tumors [two fusion negative, one FISH positive/transcript negative (485F7, Supplementary Figure 6) and one fusion positive by both FISH and RT-PCR (325E5, Supplementary Figure 6)] were analyzed by massively pair-ended sequencing to confirm the molecular results and to screen for new alterations. The analysis confirmed the lack of any abnormalities in the two fusion negative tumors and validated the presence of *MYB-NFIB* gene fusion in the fusion positive tumor. In the FISH positive/transcript negative tumor (#485F7, Figure 2A), complex alterations were observed; Figure 2B represents schematic illustration of the inter- and intra-chromosomal changes in this tumor; these included a breakage and translocation of intron-7 sequence of the *NFIB* to a 99kb upstream location of the *MYB* coding region (Supplementary Table 3) and a novel fusion between *NFIB* gene and two alternative variants of the *AIG1* gene on chromosome 6q24. The *MYB-NFIB* fusion transcript resulting from this translocation was confirmed by RT-PCR and sequencing analyses (Supplementary Figure 7).

The SNPs copy number analysis of chromosomes 6 and 9 are shown above and below the schematic illustration in Figure 2B. Comparison of the massively parallel paired-end sequencing (Supplementary Figure 6) and Affymetrix 250k SNP genomic array data confirmed that the genomic alterations occurred at copy number neutral region of chromosome 6 (Figure 2B and Supplemental Figure 8).

Combined Fusion analysis and Clinicopathologic parameters

The combined analysis of the 102 (30 new and 72 previously reported) tumors showed that 54 (52.9%) had genomic *MYB-NFIB* gene fusion, 39 (38.2%) of these formed fusion transcript and 48 (47.1%) were negative for any fusion related alterations (Supplementary Table 4). The expression of both *MYB* exon 2-3 and exon 15-16 segments in transcript forming tumors was significantly (Mann-Whitney U-test) higher than those with transcript negative tumors ($p < 0.001$ and $p = 0.003$, respectively). The expression of *MYB* exon 2-3 in tumors with only genomic fusion (by FISH) was significantly higher than in fusion transcript negative tumors ($p < 0.001$). The expression level of *MYB* transcript (exon 15-16) in fusion transcript negative tumor was not significantly different from the expression of gene fusion negative tumors (Supplementary Table 4).

MYB expression and patient survival in ACCs

We further examined the association of tumors with *MYB-NFIB* fusion with and without transcript formation and level of *MYB* expression (exon 2-3) and the clinicopathologic

Europe PMC Funders Author Manuscripts

Europe PMC Funders Author Manuscripts

factors and patients outcome. An arbitrary cut-off level of 470 for *MYB* expression was based on the upper quartile of *MYB* (exon 2-3) expression among all the samples tested. This value was used in the statistical correlative analysis. Kaplan-Meier analysis showed significant correlation between high *MYB* expression and poor survival (p=0.004 log-rank test). Univariate Cox proportional hazard regression analyses showed that high *MYB* expression, age of 60 or more years, and tumor with solid component were significant prognostic factors (Wald p=0.005 p=0.008 and p<0.001, respectively, Table 2). Interestingly, significantly different survival plot for patients with low *MYB* and solid tumors with those who had high *MYB* and solid phenotype tumors was found suggesting that high *MYB* expression correlates with poor outcome independent of the solid phenotype.

DISCUSSION

Our study identified novel and a spectrum of complex cytogenetic and molecular alterations associated with the t(6;9) event in ACC. The results show that approximately 53% of ACCs showed genomic *MYB-NFIB* fusion with and without fusion transcript formation. These findings are in agreement with those recently reported in a retrospective study of this entity (22). The majority of tumors with genomic fusion represented in-frame translocation of the *MYB* and the *NFIB* genes with the formation of variable chimeric fusion transcripts in a cell and tissue specific context (15). Interestingly, in the subset of non-transcript forming *MYB-NFIB* gene fusion tumors, we identified translocation breakpoints at the flanking sites of the *MYB* gene on chromosome 6q24 region with no evidence of *MYB* transcript alteration. Similar breakpoints at the flanking sequences of fusion genes in several neoplastic entities have also been reported (16, 17). The predicted biological consequences of these alterations are most likely the disregulation of critical oncogenes neighboring these sites (29-32).

In this study, multiple breakpoints exclusive of those reported between the *MYB* and the *NFIB* genes were identified. These included translocations involving, exon 15 of *MYB* and intron 3 of the *PDCD1LG2* gene on chromosome 9p24 and *MYB* exon 13, intron 22 of the *EFR3A* gene on chromosome 8q24 (16, 33, 34) and the *NFIB* with the *AIG1* on chromosome 6q24. In addition, a separate intragenic translocation of an *NFIB* sequence to a proximal site of the *MYB* coding region was also identified in the latter tumor. The translocation involving intron sites in these instances have previously been reported in a benign *(HMGA2* and *COG5)* (34) (*NFIB* and to the *HMGA2* gene) (36-40) and malignant tumors (*EML4-ALK* fusion gene) (40, 41). The mechanistic association of these uncommon events in the oncogenesis of ACC, however, remains to be elucidated.

Our findings strongly link the *MYB-NFIB* gene fusion to the upregulation of the *MYB* gene in ACCs. This may likely be due either to the lack of the 3′UTR, which includes the regulatory microRNA target sites, or to the deletion of the terminal negative regulatory domain (NRD) of the *MYB* fusion transcript positive ACCs. The translocation of other genetic sequences to the non-coding flanking sites of the *MYB* gene can also lead to the *MYB* transcriptional activation perhaps through epigenetic modification including histone acetylation especially in *MYB-NFIB* fusion transcript negative tumors. (19, 21, 23, 34, 43). Other upstream events affecting the transcription of the *MYB* gene in fusion transcript negative tumors including (43) the *NFIB* sequence translocation upstream of the coding region leading to high *MYB* expression can be involved. Interestingly, our findings are distinctly different from those associated with the activation of this gene in other solid tumors including colon (19, 36, 44) and breast carcinomas and suggest that *MYB* regulation varies in a tissue and tumor specific context. (33, 34, 37, 38, 42, 45-48)

In this study, clinicopathologic analysis identified three factors including patients older than 60 years, solid phenotype and high *MYB* expression to be significantly associated with poor

Europe PMC Funders Author Manuscripts

survival. In both, multi-factorial cox hazard ratio, log-rank testing and the survival plot for patients with low *MYB* and solid type was significant different from patients with high *MYB* and solid type. We contend, however, that further studies are required to assess the functional threshold of *MYB* expression, to identify chimeric fusion protein and to determine the significance of the selective *MYB* expression to myoepithelial cells in the pathobiology of ACC. These studies will be further advanced by the availability of reagents that distinguish between the *MYB* protein variants as well as results from second generation deep sequencing of these tumors. Overall, the data indicates that the juxtaposition of the terminal sequences of the *NFIB* within and around the coding *MYB* gene sequence is the main genetic event in the t(6;9) positive ACCs and this leads to an elevated 5′ segment of the *MYB* gene in ACC. (31, 32, 49)

In conclusion, we comprehensively accounted for the alternative *MYB-NFIB* gene fusions and the other molecular-genetic alterations associated with the t(6;9) in ACCs and showed that marked genetic heterogeneity are associated with this event. The study characterized two main events resulting from the t(6;9) one with gene fusion alone and another with gene fusion and chimeric transcript formation. The former is due to breakpoints at the flanking sites of the *MYB* gene. These alterations require multiple methodological approaches for their detection. The results also show that transcript forming ACCs express high 5′-truncated *MYB* segment and pursue aggressive behavior. We therefore contend that the translocation of the *NFIB* terminal sequences as a result of the t(6;9) and different molecular events, may underlie the transcriptional regulation of the *MYB* gene in ACC.

Supplementary Material

Refer to Web version on PubMed Central for supplementary material.

Acknowledgments

The authors are grateful to Dr. Scott A. Ness for update information on the *MYB* gene and to Deborah A. Rodriguez and Stella U. Njoku for technical and Wendy Garcia for secretarial assistance.

GRANT SUPPORT:

The study is supported in part by the NIH National Institute of Dental and Craniofacial Research (NIDCR) and the NIH Office of Rare Diseases Research (ORDR) Grant Number U01DE019765, the Head and Neck SPORE program Grant Number P50 CA097007, The Kenneth D. Muller professorship and the NCI-CA-16672 grant. AF and PS acknowledge the support of the Wellcome Trust under grant reference number 077012/Z/05/Z. The content is solely the responsibility of the authors and does not necessarily represent the official views of the National Cancer Institute or the National Institute of Health.

REFERENCES

1. Batsakis JG, Regezi JA, Luna MA, El-Naggar AK. Histogenesis of salivary gland neoplasms: a postulate with prognostic implications. J Laryngol Otol. 1989; 103:939–44. [PubMed: 2685148]
2. Batsakis JG, Luna MA, El-Naggar AK. Histopathologic grading of salivary gland neoplasms: III. Adenoid cystic carcinomas. Ann Otol Rhinol Laryngol. 1990; 99:1007–9. [PubMed: 2173892]
3. Chomette G, Auriol M, Tranbaloc P, Vaillant JM. Adenoid cystic carcinoma of minor salivary glands. Analysis of 86 cases. Clinico-pathological, histoenzymological and ultrastructural studies. Virchows Arch A Pathol Anat Histol. 1982; 395:289–301. [PubMed: 6287713]
4. Spiro RH. Salivary neoplasms: overview of a 35-year experience with 2,807 patients. Head Neck Surg. 1986; 8:177–84. [PubMed: 3744850]
5. Fordice J, Kershaw C, El-Naggar AK, Goepfert H. Adenoid cystic carcinoma of the head and neck: predictors of morbidity and mortality. Arch Otolaryngol Head Neck Surg. 1999; 125:149–52. [PubMed: 10037280]

Europe PMC Funders Author Manuscripts

Europe PMC Funders Author Manuscripts

6. El-Naggar, AK.; Huvos, AG. Adenoid cystic carcinoma. In: Barnes, L.; Eveson, JW.; Reichart, P.; Sidransky, D., editors. World Health Organization Classification of Tumors Pathology and Genetics of Head and Neck Tumors. IARC Press; Lyon, France: 2005. p. 221-2.
7. Bell D, Zhao YJ, Rao PH, Weber RS, El-Naggar AK. Translocation t(6;14) as the sole chromosomal abnormality in adenoid cystic carcinoma of the base of tongue. Head Neck Pathol. 2007; 1:165–8. [PubMed: 20614269]
8. Higashi K, Jin Y, Johansson M, Heim S, Mandahl N, Biorklund A, et al. Rearrangement of 9p13 as the primary chromosomal aberration in adenoid cystic carcinoma of the respiratory tract. Genes Chromosomes Cancer. 1991; 3:21–3. [PubMed: 1648955]
9. Frierson HF Jr. El-Naggar AK, Welsh JB, Sapinoso LM, Su AI, Cheng J, et al. Large scale molecular analysis identifies genes with altered expression in salivary adenoid cystic carcinoma. Am J Pathol. 2002; 161:1315–23. [PubMed: 12368205]
10. Rutherford S, Hampton GM, Frierson HF, Moskaluk CA. Mapping of candidate tumor suppressor genes on chromosome 12 in adenoid cystic carcinoma. Lab Invest. 2005; 85:1076–85. [PubMed: 16025147]
11. Queimado L, Reis A, Fonseca I, Martins C, Lovett M, Soares J, et al. A refined localization of two deleted regions in chromosome 6q associated with salivary gland carcinomas. Oncogene. 1998; 16:83–8. [PubMed: 9467946]
12. Stallmach I, Zenklusen P, Komminoth P, Schmid S, Perren A, Roos M, et al. Loss of heterozygosity at chromosome 6q23-25 correlates with clinical and histologic parameters in salivary gland adenoid cystic carcinoma. Virchows Arch. 2002; 440:77–84. [PubMed: 11942580]
13. Rao PH, Roberts D, Zhao YJ, Bell D, Harris CP, Weber RS, et al. Deletion of 1p32-p36 is the most frequent genetic change and poor prognostic marker in adenoid cystic carcinoma of the salivary glands. Clin Cancer Res. 2008; 14:5181–7. [PubMed: 18698036]
14. Persson M, Andren Y, Mark J, Horlings HM, Persson F, Stenman G. Recurrent fusion of *MYB* and *NFIB* transcription factor genes in carcinomas of the breast and head and neck. Proc Natl Acad Sci U S A. 2009; 106:18740–4. [PubMed: 19841262]
15. Mitani Y, Li J, Rao PH, Zhao YJ, Bell D, Lippman SM, et al. Comprehensive analysis of the *MYB-NFIB* gene fusion in salivary adenoid cystic carcinoma: Incidence, variability, and clinicopathologic significance. Clin Cancer Res. 2010; 16:4722–31. [PubMed: 20702610]
16. Clappier E, Cuccuini W, Kalota A, Crinquette A, Cayuela JM, Dik WA, et al. The C-*MYB* locus is involved in chromosomal translocation and genomic duplications in human T-cell acute leukemia (T-ALL), the translocation defining a new T-ALL subtype in very young children. Blood. 2007; 110:1251–61. [PubMed: 17452517]
17. Tomita A, Watanabe T, Kosugi H, Ohashi H, Uchida T, Kinoshita T, et al. Truncated c-*MYB* expression in the human leukemia cell line TK-6. Leukemia. 1998; 12:1422–9. [PubMed: 9737692]
18. Harper ME, Franchini G, Love J, Simon MI, Gallo RC, Wong-Staal F. Chromosomal sublocalization of human c-*MYB* and c-fes cellular onc genes. Nature. 1983; 304:169–71. [PubMed: 6866112]
19. Ramsay RG, Gonda TJ. *MYB* function in normal and cancer cells. Nat Rev Cancer. 2008; 8:523–34. [PubMed: 18574464]
20. Nomura N, Takahashi M, Matsui M, Ishii S, Date T, Sasamoto S, et al. Isolation of human cDNA clones of *MYB*-related genes, A-*MYB* and B-*MYB*. Nucleic Acids Res. 1988; 16:11075–89. [PubMed: 3060855]
21. Bellon T, Perrotti D, Calabretta B. Granulocytic differentiation of normal hematopoietic precursor cells induced by transcription factor PU.1 correlates with negative regulation of the c-*MYB* promoter. Blood. 1997; 90:1828–39. [PubMed: 9292515]
22. West RB, Kong C, Clarke N, Gilks T, Lipsick JS, Cao H, et al. *MYB* expression and translocation in adenoid cystic carcinomas and other salivary gland tumors with clinicopathologic correlation. Am J Surg Pathol. 2011; 35:92–9. [PubMed: 21164292]
23. Dubendorff JW, Lipsick JS. Transcriptional regulation by the carboxyl terminus of c-*MYB* depends upon both the *MYB* DNA-binding domain and the DNA recognition site. Oncogene. 1999; 18:3452–60. [PubMed: 10376523]

Europe PMC Funders Author Manuscripts

Europe PMC Funders Author Manuscripts

24. Campbell PJ, Yachida S, Mudie LJ, Stephens PJ, Pleasance ED, Stebbings LA, et al. The patterns and dynamics of genomic instability in metastatic pancreatic cancer. Nature. 2010; 467:1109–13. [PubMed: 20981101]
25. Stephens PJ, McBride DJ, Lin ML, Varela I, Pleasance ED, Simpson JT, et al. Complex landscapes of somatic rearrangement in human breast cancer genomes. Nature. 2009; 462:1005–10. [PubMed: 20033038]
26. Li H, Ruan J, Durbin R. Mapping short DNA sequencing reads and calling variants using mapping quality scores. Genome Res. 2008; 18:1851–8. [PubMed: 18714091]
27. Zhou YE, O'Rourke JP, Edwards JS, Ness SA. Single molecular analysis of c-*MYB* alternative splicing reveals novel classifiers for precursor B-ALL. PLoS One. 2011:e22880. [PubMed: 21853052]
28. Stephens PJ, Greenman CD, Fu B, Yang F, Bignell GR, Mudie LJ, et al. Massive genomic rearrangement acquired in a single catastrophic event during cancer development. Cell. 2011; 144:27–40. [PubMed: 21215367]
29. Collins EC, Rabbitts TH. The promiscuous MLL gene links chromosomal translocations to cellular differentiation and tumour tropism. Trends Mol Med. 2002; 8:436–42. [PubMed: 12223315]
30. Lastowska M, Roberts P, Pearson AD, Lewis I, Wolstenholme J, Bown N. Promiscuous translocations of chromosome arm 17q in human neuroblastomas. Genes Chromosomes Cancer. 1997; 19:143–9. [PubMed: 9218994]
31. Butler MP, Iida S, Capello D, Rossi D, Rao PH, Nallasivam P, et al. Alternative translocation breakpoint cluster region 5′ to BCL-6 in B-cell non-Hodgkin's lymphoma. Cancer Res. 2002; 62:4089–94. [PubMed: 12124346]
32. Chen W, Butler M, Rao PH, Chaganti SR, Louie DC, Dalla-Favera R, et al. The t(2;3)(q21;q27) translocation in non-Hodgkin's lymphoma displays BCL6 mutations in the 5′ regulatory region and chromosomal breakpoints distant from the gene. Oncogene. 1998; 17:1717–22. [PubMed: 9796700]
33. Catchpole S, Tavner F, Le Cam L, Sardet C, Watson RJ. A B-*MYB* promoter corepressor site facilitates in vivo occupation of the adjacent E2F site by p107 × E2F and p130 × E2F complexes. J Biol Chem. 2002; 277:39015–24. [PubMed: 12147683]
34. Nicolaides NC, Gualdi R, Casadevall C, Manzella L, Calabretta B. Positive autoregulation of c-*MYB* expression via *MYB* binding sites in the 5′ flanking region of the human c-*MYB* gene. Mol Cell Biol. 1991; 11:6166–76. [PubMed: 1944282]
35. Velagaleti GV, Tonk VS, Hakim NM, Wang X, Zhang H, Erickson-Johnson MR, et al. Fusion of HMGA2 to COG5 in uterine leiomyoma. Cancer Genet Cytogenet. 2010; 202:11–6. [PubMed: 20804914]
36. Drabsch Y, Hugo H, Zhang R, Dowhan DH, Miao YR, Gewirtz AM, et al. Mechanism of and requirement for estrogen-regulated *MYB* expression in estrogen-receptor-positive breast cancer cells. Proc Natl Acad Sci U S A. 2007; 104:13762–7. [PubMed: 17690249]
37. Trauth K, Mutschler B, Jenkins NA, Gilbert DJ, Copeland NG, Klempnauer KH. Mouse A-*MYB* encodes a trans-activator and is expressed in mitotically active cells of the developing central nervous system, adult testis and B lymphocytes. EMBO J. 1994; 13:5994–6005. [PubMed: 7813437]
38. Stenman G. Fusion oncogenes and tumor type specificity--insights from salivary gland tumors. Semin Cancer Biol. 2005; 15:224–35. [PubMed: 15826837]
39. Mitelman F, Johansson B, Mertens F. Fusion genes and rearranged genes as a linear function of chromosome aberrations in cancer. Nat Genet. 2004; 36:331–4. [PubMed: 15054488]
40. Rabbitts TH. Chromosomal translocations in human cancer. Nature. 1994; 372:143–9. [PubMed: 7969446]
41. Nagel S, Kaufmann M, Scherr M, Drexler HG, MacLeod RA. Activation of HLXB9 by juxtaposition with *MYB* via formation of t(6;7)(q23;q36) in an AML-M4 cell line (GDM-1). Genes Chromosomes Cancer. 2005; 42:170–8. [PubMed: 15540222]
42. Sinclair P, Harrison CJ, Jarosova M, Foroni L. Analysis of balanced rearrangements of chromosome 6 in acute leukemia: clustered breakpoints in q22-q23 and possible involvement of c-

MYB in a new recurrent translocation, t(6;7)(q23;q32 through 36). Haematologica. 2005; 90:602–11. [PubMed: 15921375]

43. Mukai HY, Motohashi H, Ohneda O, Suzuki N, Nagano M, Yamamoto M. Transgene insertion in proximity to the c-*MYB* gene disrupts erythroid-megakaryocytic lineage bifurcation. Mol Cell Biol. 2006; 26:7953–65. [PubMed: 16940183]
44. Thompson MA, Flegg R, Westin EH, Ramsay RG. Microsatellite deletions in the c-*MYB* transcriptional attenuator region associated with over-expression in colon tumour cell lines. Oncogene. 1997; 14:1715–23. [PubMed: 9135073]
45. Brenner JC, Chinnaiyan AM. Translocations in epithelial cancers. Biochim Biophys Acta. 2009; 1796:201–15. [PubMed: 19406209]
46. Aplan PD. Causes of oncogenic chromosomal translocation. Trends Genet. 2006; 22:46–55. [PubMed: 16257470]
47. Biroccio A, Benassi B, Agnano I, D'Angelo C, Buglioni S, Mottolese M, et al. c-*MYB* and Bcl-x overexpression predicts poor prognosis in colorectal cancer: clinical and experimental findings. Am J Pathol. 2001; 158:1289–99. [PubMed: 11290547]
48. Rabbitts TH, Stocks MR. Chromosomal translocation products engender new intracellular therapeutic technologies. Nat Med. 2003; 9:383–6. [PubMed: 12669051]
49. Kauraniemi P, Hedenfalk I, Persson K, Duggan DJ, Tanner M, Johannsson O, et al. *MYB* oncogene amplification in hereditary BRCA1 breast cancer. Cancer Res. 2000; 60:5323–8. [PubMed: 11034064]

Europe PMC Funders Author Manuscripts

Europe PMC Funders Author Manuscripts

Europe PMC Funders Author Manuscripts

Europe PMC Funders Author Manuscripts

Statement of Translational Relevance

This study identifies previously unreported chromosomal breakpoints and complex genetic and molecular alterations associated with the t(6;9) in salivary adenoid cystic carcinoma (ACC). These events result in *MYB-NFIB* gene fusion with and without chimeric transcript formation. Tumors with *MYB-NFIB* gene fusion without transcript had the translocation of terminal sequences of the *NFIB* to the flanking sites of the *MYB* gene. Gene fusion resulting in transcript formation was associated with high level expression of the *MYB* 5′ segment and significantly correlated with patients' survival. The study provides detailed characterization of the t(6;9) alterations and their link to *MYB* expression in an effort to define targets for therapeutic stratification of patients with ACC.

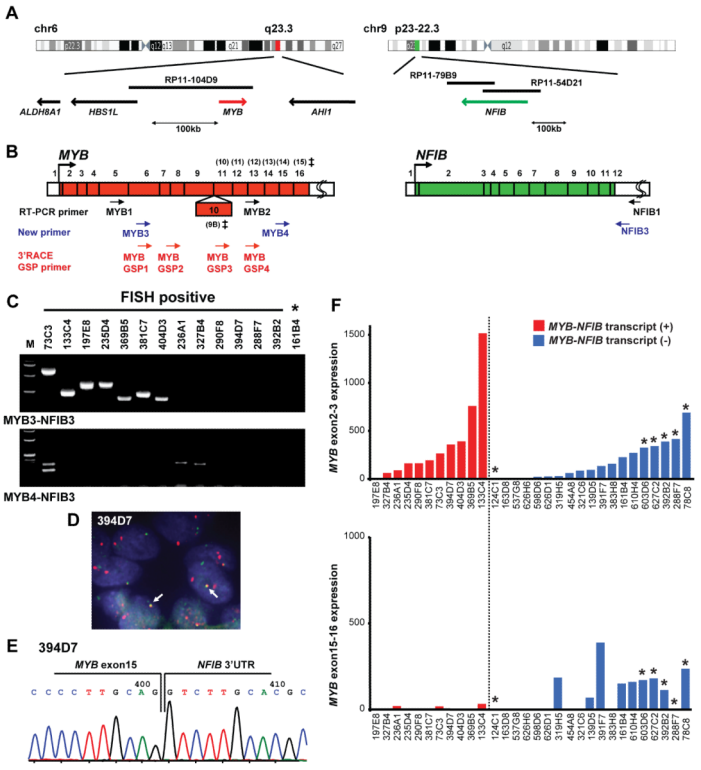

Figure 1.

A) Schematic representation of the location of the *MYB* chromosome 6q23 and the *NFIB* on 9p22-23 and the BAC clones used for the FISH analysis. RP11-104D9 was used as a probe for *MYB* and probes RP11-79B and RP11-54D21 were used for the *NFIB* gene in the FISH analysis. B) Schematic structure of the *MYB* and the *NFIB* genes and the primers used for the RT-PCR and the 3′RACE analysis. The exon numbers of *MYB* are based on NCBI database (accession number NM_001130173). *NFIB* exon numbers were obtained from accession number ENSG0000147862 for *NFIB* in the Ensembl database; note *MYB* exon 10 is not included any *MYB-NFIB* chimeric transcripts and intact *MYB*. ‡*MYB* exon 10 is also known well as exon 9B (accession number HSU22376).

C) RT-PCR analysis of *MYB-NFIB* fusion transcripts using new primer sets. Asterisk points to case #161B4 where gene fusion was detected by FISH without transcript formation. D) FISH analysis using BAC clones of *MYB* (green) and *NFIB* (red) genes in transcript negative gene fusion positive ACC (394D7 case). White arrows point to the yellow signal representing the *MYB* and *NFIB* gene fusion. E) Sequence illustration shows fusion of *MYB* exon 15 with *NFIB* 3′UTR, as detected by 3′RACE in 394D7 case. F) Represents the *MYB* transcript expression of the 30 new cases. The red bars denote the *MYB-NFIB* transcript positive samples, whereas the blue bars represent the expression level in fusion negative tumors. The asterisks point to tumors with *MYB/NFIB* gene fusion by FISH only. Results are represented as fold increase relative to *MYB* expression in pooled normal salivary gland tissue.

Europe PMC Funders Author Manuscripts
Europe PMC Funders Author Manuscripts

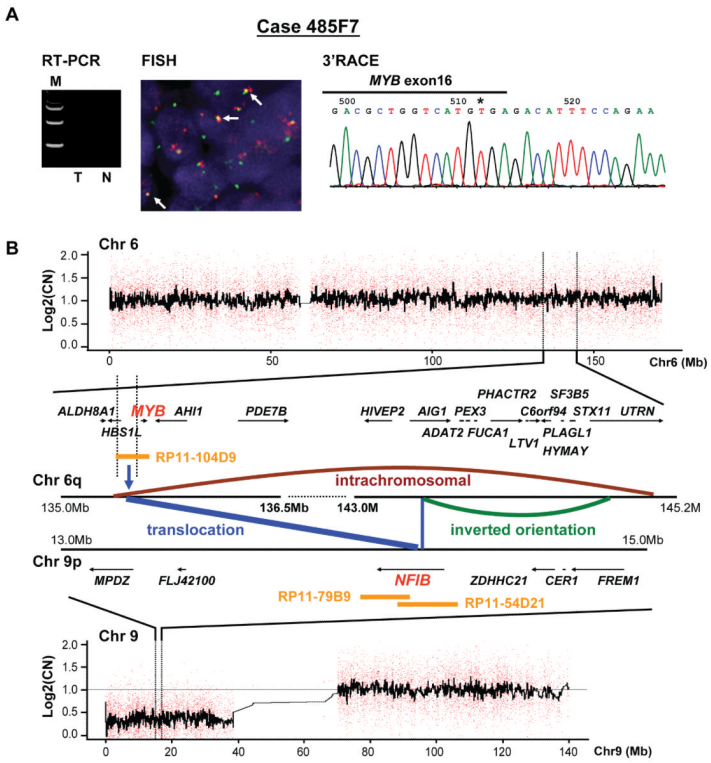

Figure 2.

The chromosomal rearrangements in case 485F7, as an example of genomic *MYB-NFIB* fusion without transcript formation. A) RT-PCR analysis shows as *MYB-NFIB* transcript negative (T) and corresponding normal (N). The 3′RACE analysis reveals that the last exon 16 of *MYB* gene is intact. B) Genomic rearrangement and copy number changes of chromosomes 6 and 9 of the same tumor. The center schematic representation depicts the intra- and inter-chromosomal structures generated from the massively pared-end tag sequencing data. Blue bars, chromosomal rearrangement (*MYB-NFIB* and *NFIB-AIG1*); brown bar, intra-chromosomal rearrangement between *HBS1L* and *UTRN* gene; green bar, inverted orientation between *AIG1* and *UTRN* gene. Blue vertical arrow indicates *NFIB* gene breaks at intron 7 that translocates to chromosome 6q22 just proximal to the *MYB* upstream. *MYB* probe (RP11-104D9) and *NFIB* probe (RP11-79B and RP11-54D21) are shown as FISH probes.

Europe PMC Funders Author Manuscripts
Europe PMC Funders Author Manuscripts

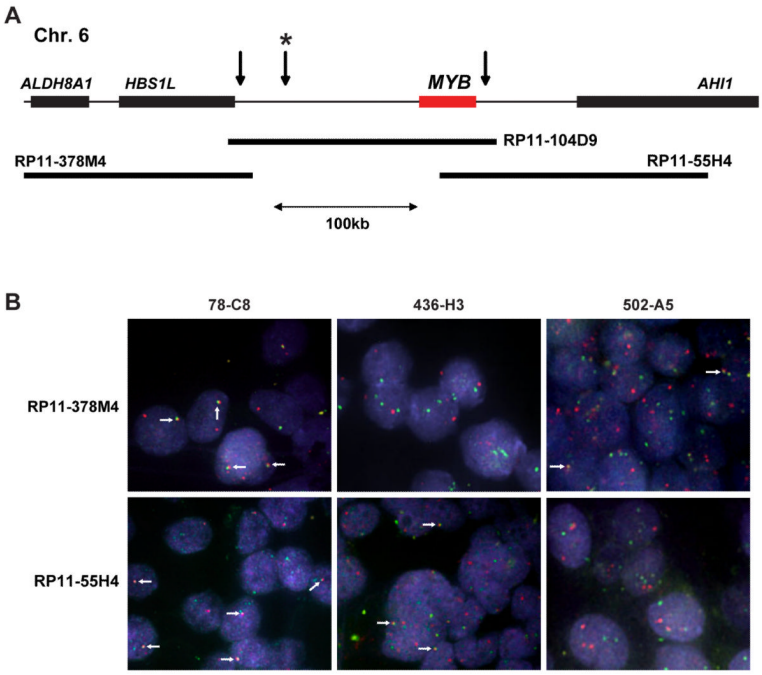

Figure 3.

Alternative breakpoint in the proximal or the distal sites of the *MYB* gene. A) The schematic representation of FISH probe for *MYB* gene displays the overlapping of RP11-378M and RP11-55H4 probes with the initial screening probe (RP11-104D9). The arrows showed the break point locations, and the asterisk means a breakage at 99kb upstream of *MYB* gene in 485F7 samples. B) The white arrows point to a yellow signal representing the t(6;9) translocation. Case 78 is positive for both.

Europe PMC Funders Author Manuscripts
Europe PMC Funders Author Manuscripts

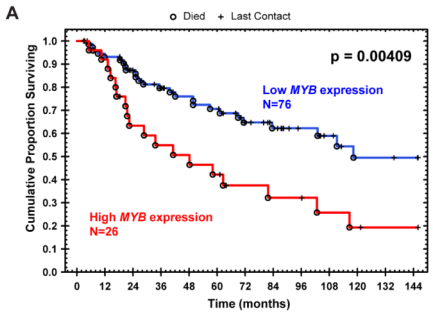

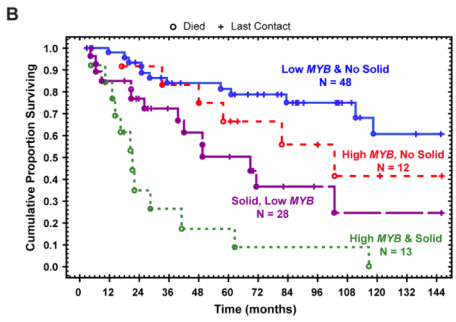

two sided log-rank test *p* value				
Factor(s)	Low *MYB* & No solid	High *MYB*, No solid	Solid , Low *MYB*	High *MYB* & Solid
Low *MYB* & No solid	NA	0.209	0.005	<0.001
High *MYB*, No Solid	0.209	NA	0.216	0.002
Solid, Low *MYB*	0.005	0.216	NA	0.015
High *MYB* & Solid	<0.001	0.002	0.015	NA

Figure 4.

Kaplan-Meier survival curves of ACCs patients: A) correlation between high *MYB* exon 2-3 expression and poor patient survival (p=0.004, log-rank test). B) survival curves of *MYB* transcript expression, Adenoid Cystic Carcinoma with solid component and patients survival.

Europe PMC Funders Author Manuscripts

Europe PMC Funders Author Manuscripts

Europe PMC Funders Author Manuscripts
Europe PMC Funders Author Manuscripts

Table 1

Molecular and Genetic results of the 30 new Adenoid Cystic Carcinomas

Sample Number	*MYB-NFIB* (new primer)	3'RACE[a]	FISH	Q-PCR_MYB	
				(exon 2-3)	(exon 15-16)
197-E8	*MYB* exon 9b- *NFIB* exon 11 *MYB* exon 9b- *NFIB* exon 12	N.P.	+	10	1
327-B4	*MYB* exon15- *NFIB* exon 12	*MYB* exon 15- *NFIB* exon 12	+	62	0
236-A1	*MYB* exon 15- *NFIB* exon 12	*MYB* exon 15- *NFIB* exon 12 *MYB* exon 15- *NFIB* exon 11	+	90	20
235-D4	*MYB* exon 9b- *NFIB* exon 11 *MYB* exon 9b- *NFIB* exon 12	N.P.	+	161	5
290-F8	-	*MYB* exon 15- *NFIB* 3'UTR	+	162	1
381-C7	*MYB* exon 8b- *NFIB* exon 11	N.P.	+	194	0
73-C3	*MYB* exon 15- *NFIB* exon 12 *MYB* exon 15- *NFIB* exon 11	N.P.	+	266	18
394-D7	-	*MYB* exon 15- *NFIB* 3'UTR	+	358	0
404-D3	*MYB* exon 8b- *NFIB* exon 12	N.P.	+	392	0
369-B5	*MYB* exon 8b- *NFIB* exon 12	N.P.	+	760	4
133-C4	*MYB* exon 8b- *NFIB* exon 12	N.P.	+	1516	33
163-D8	-	N.P.	−	0	0
537-G8	-	N.P.	−	0	1
124-C1	-	N/A	+	0	0
626-H6	-	N.P.	−	3	1
598-D6	-	N.P.	−	22	0
626-D1	-	N.P.	−	25	0
319-H5	-	N.P.	−	30	185
454-A8	-	N.P.	−	62	1
321-C6	-	N.P.	−	86	0
139-D5	-	N.P.	−	93	69
391-F7	-	N/A	−	133	388
383-H8	-	N/A	−	158	80
161-B4	-	N/A	−	226	150

Clin Cancer Res. Author manuscript; available in PMC 2012 May 15.

Europe PMC Funders Author Manuscripts

Europe PMC Funders Author Manuscripts

Sample Number	*MYB-NFIB* (new primer)	3'RACE[a]	FISH	Q-PCR_MYB	
				(exon 2-3)	(exon 15-16)
610-H4	-	N/A	+	271	160
603-D6	-	N.P.	−	326	171
627-C2	-	N/A	+	342	180
392-B2	-	N/A	+	388	113
288-F7	-	*MYB* exon 13- *MYB* intron 13- *EFR3A* intron 22 (Chr8q24.22)	+	416	6
78-C8	-	N/A	+	691	237

Molecular genetic results of the subset of ACC with alterations from previous study.

Sample Number	*MYB-NFIB* (new primer)	3'RACE[a]	FISH	Q-PCR_*MYB*	
				(exon 2-3)	(exon 15-16)
405-B2	-	*MYB* exon 15- *PDCDILG2* (chr 9; intron 3, inversion)	+	106	0
[b]485-F7	-	N/A	+	231	421
233-C2	-	N/A	+	177	188
526-B5	-	N/A	+	368	213
471-F2	-	N/A	+	105	288
484-H3	-	N/A	+	105	213
594-D3	-	N/A	+	128	34
542-A1	-	*MYB* exon 14- *NFIB* 3'UTR	+	881	29
502-A5	-	N/A	+	606	384
185-G8	*MYB* exon 11- *NFIB* exon 12	*MYB* exon 11- *NFIB* exon 12	+	1264	635
335-C6	*MYB* exon 8b- *NFIB* exon 12	*MYB* exon 8b- *NFIB* exon 12	+	1229	5
191-D6	*MYB* exon11- *NFIB* exon 12	*MYB* exon 11- *NFIB* exon 12	+	488	62
318-H3	-	*MYB* exon/intron 11- *NFIB* 3'UTR	+	0	0
391-D6	*MYB* exon 12- *NFIB* exon 11	*MYB* exon 15- *NFIB* exon 11	+	23	0
436-E2	*MYB* exon 8a- *NFIB* exon 12 *MYB* exon 8a- *NFIB* exon 11	*MYB* exon 8a- *NFIB* exon 12	+	1217	5
436-H3	-	N/A	+	229	476
570-H7	*MYB* exon 8a- *NFIB* exon 12	*MYB* exon 8a- *NFIB* exon 12	+	446	0

Europe PMC Funders Author Manuscripts

Europe PMC Funders Author Manuscripts

Note:

Note:

[a] N.P., not performed; N/A, No-Abnormality (*MYB* gene is intact at 3'region). (−), negative; (+), positive.

[a] N/A, No-Abnormality (*MYB* gene is intact at 3'region). (−), negative; (+), positive.

[b] 485-F7 sample had a *NFIB-AIG1* gene fusion

Europe PMC Funders Author Manuscripts
Europe PMC Funders Author Manuscripts

Clin Cancer Res. Author manuscript; available in PMC 2012 May 15.

Table 2

Multifactorial (Cox) regression analysis of factors affecting 12-year overall survival of ACC patients

Variable	No.	Univariate analysis HR (95% CI)	p[a]	Multivariate analysis[c] HR (95% CI)	p[a]
***MYB-NFIB* transcript**					
negative	63	1.00	0.12	N/A	N/A
positive	39	1.602 (0.892-2.844)			
FISH					
negative	48	1.00	0.07	N/A	N/A
positive	54	1.734 (0.947-3.173)			
***MYB* expression (exon2-3)** [b]					
Low	76	1.00	0.005	1.00	0.014
High	26	1.003 (1.001-1.005)		1.003 (1.001-1.005)	
Age					
<60	67	1.00	0.008	1.00	0.008
≥60	35	1.057 (1.016-1.100)		1.055 (1.014-1.097)	
Gender					
Female	41	1.00	0.64	N/A	N/A
Male	61	1.154 (0.639-2.087)			
Size					
<4cm	63	1.00	0.94	N/A	N/A
≥4cm	35	0.987 (0.723-1.349)			
Pattern					
Not Solid	60	1.00	<0.001	1.00	<0.001
Solid	41	3.706 (2.027-6.777)		3.596 (1.963-6.589)	
PNI					
No	7	1.00	0.58	N/A	N/A

Europe PMC Funders Author Manuscripts

Europe PMC Funders Author Manuscripts

Variable	No.	Univariate analysis HR (95% CI)	p[a]	Multivariate analysis[c] HR (95% CI)	p[a]
Yes	78	1.499 (0.361-6.229)			
Stage [c]					
I-II	20	1.00	0.14	N/A	N/A
III-IV	35	1.919 (2.027-6.777)			
Metastasis					
No	50	1.00	0.97	N/A	N/A
Yes	52	1.012 (0.564-1.817)			

Overall Model, p<0.00001. N/A = not applicable

PNI: Perineural invasion

[a]Wald p-value.

[b]470 was defined as a cut-off value for *MYB* expression (exon2-3).

[c]55 patients are available for the staging analysis.